



Direct 3D printed shadow mask on Silicon

Downloaded from: <https://research.chalmers.se>, 2024-08-16 22:22 UTC

Citation for the original published paper (version of record):

Rahiminejad, S., Köhler, E., Enoksson, P. (2016). Direct 3D printed shadow mask on Silicon. *Journal of Physics: Conference Series*, 757(1). <http://dx.doi.org/10.1088/1742-6596/757/1/012021>

N.B. When citing this work, cite the original published paper.

PAPER • OPEN ACCESS

Direct 3D printed shadow mask on Silicon

To cite this article: S Rahiminejad *et al* 2016 *J. Phys.: Conf. Ser.* **757** 012021

View the [article online](#) for updates and enhancements.

You may also like

- [Shadow mask assisted direct growth of ZnO nanowires as a sensing medium for surface acoustic wave devices using a thermal evaporation method](#)
Ajay Achath Mohanan, R Parthiban and N Ramakrishnan
- [Optimum reactive ion etching of x-cut quartz using SF₆ and Ar](#)
M D Minnick, G A Devenyi and R N Kleiman
- [Deposition and patterning of electrodes on the vertical sidewalls of deep trenches](#)
L Bonnin, A Plot, N Isac et al.



PRIMETM
PACIFIC RIM MEETING
ON ELECTROCHEMICAL
AND SOLID STATE SCIENCE
HONOLULU, HI
October 6-11, 2024

Joint International Meeting of
The Electrochemical Society of Japan (ECSJ)
The Korean Electrochemical Society (KECS)
The Electrochemical Society (ECS)

Early Registration Deadline:
September 3, 2024

**MAKE YOUR PLANS
NOW!**

Direct 3D printed shadow mask on Silicon

S Rahiminejad, E Köhler and P Enoksson

Chalmers University of Technology, Department of Micro and Nanotechnology, Sweden

E-mail: rahimine@chalmers.se

Abstract. A 3D printed shadow mask method is presented. The 3D printer prints ABS plastic directly on the wafer, thus avoiding gaps between the wafer and the shadow mask, and deformation during the process. The wafer together with the 3D printed shadow mask was sputtered with Ti and Au. The shadow mask was released by immersion in acetone. The sputtered patches through the shadow mask were compared to the opening of the 3D printed shadow mask and the design dimensions. The patterned Au patches were larger than the printed apertures, however they were smaller than the design widths. The mask was printed in 4 min, the cost is less than one euro cent, and the process is a low temperature process suitable for temperature sensitive components.

1. Introduction

One of the most important steps during microfabrication is masking of the wafer. There exists different masking techniques, the most common one is photolithography.

Photolithography can be done by writing the pattern into the photoresist with e.g. an e-beam or a laser writer. Photolithography can also be done with a chrome mask placed between the photoresist covered wafer and a UV light source.

When patterning metal, Lift-off is a method that avoids etching of the metal. This process masks a negative photoresist pattern, which is then covered with the metal. The photoresist is then removed with a solvent, together with the metal on top of the photoresist. One issue with photoresist masking is that some photoresist development solvents can etch exposed metal surfaces on the wafer.

Another masking technique is when a shadow mask is used. The first shadow mask was presented in 1986 [1]. A shadow mask is a mechanical mask that can be used for metal patterning [2, 3, 4] similar to lift-off or as a hard mask during plasma etching [5], and also for polymer spray coating [6]. They can be active, that is that the aperture openings can be adjusted, or passive with fixed aperture sizes. Metal shadow masks made by milling are suitable for larger aperture sizes, laser cutting can be used to create smaller aperture sizes. However, when high resolution micro-aperture sizes are needed, microfabricated shadow masks are used. Microfabricated shadow masks are often made out of Si [2, 3, 4, 5], where a Si wafer is patterned with photolithography and the aperture is etched either by wet or dry etching. These shadow masks are then clamped [2, 5] or taped with heat resistive tape. In [6] a different kind of shadow mask made out of Ni with a novel magnetic clamping method was presented. However, all of the presented shadow masks still needs a photolithography step and an etch step to create the shadow mask.

3D printing can produce shadow masks rapidly and at a low cost compared to standard shadow masks, partly because no photolithography and etch step is needed, and mostly because the printing time is within minutes and material cost is low. In [7, 8] 3D printed shadow masks are used. However these shadow masks still needs to be attached to the substrate with either heat resistive tape or with an alignment fixture. If the shadow mask is not in full contact with the substrate and there is an air gap



between the shadow mask and the substrate, the transferred pattern can become much wider than wanted, and deformed in the deposition chamber.

In this paper we present a 3D printed shadow lift-off mask, printed directly onto the Si wafer. This way the shadow mask is in full contact with the wafer and there are no air gaps between the shadow mask and the wafer. The ABS shadow mask is released with acetone which does not etch any metals. The printing process is done at a low cost, low temperature and at a rapid pace.

2. Shadow mask design

The shadow mask design was done with google sketchup and then exported to the 3D printer. The shadow mask has 4 x 6 apertures. The first row consist of six squares with the widths (from left to right) 2 mm, 1.8 mm, 1.6 mm, 1.4 mm, 1.2 mm and 1 mm, the second rows consists of circles with the same sized dimensions, and these rows are then repeated once more see Fig. 1.

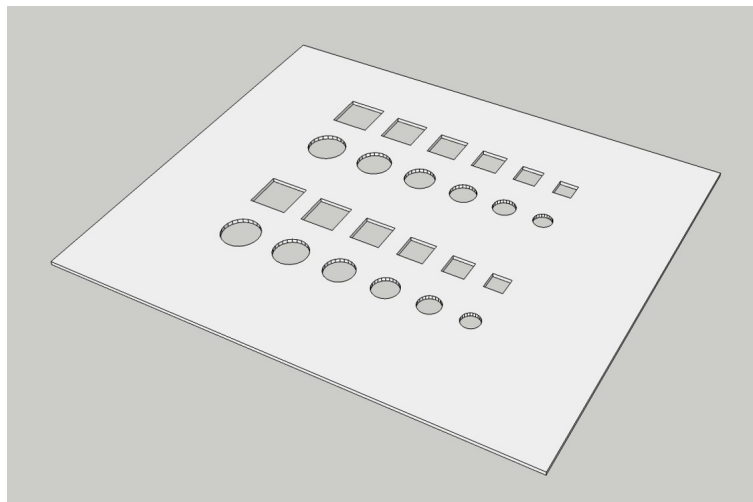


Figure 1: The mask design in google sketchup.

3. Development of 3D shadow mask

The 3D printer used was a Fused Deposition Modelling (FDM) in house built Delta 3D printer. The FDM 3D printer uses hot liquefied thermoplastic that quickly cools down and solidifies, making it possible to print the next layer on top of the previous one. The first layer can be printed on most types of materials and the adhesive properties can be improved by heating up the material. The Si wafer can be placed on the heated bed directly under the nozzle. 3D printing systems such as Selective Laser Sintering (SLS), which are powder based, are expensive and the 3D print will not attach to the Si wafer. Direct light processing (DLP) 3D printers have a limited amount of materials that can be used and the printing is done by printing the layers under the previous cured layers in a liquid. This method is not suitable since the Si wafer cannot be placed anywhere in the 3D printer.

With the in house built FDM 3D printer the x-y-z movements are smooth due to non-backlash magnetic joints and 2.5 μm step size on the stepper motors. What affects the resolution of the print is mainly the nozzle size, the nozzle temperature, the feed rate of the polymer and the speed of the nozzle head. A limitation with the FDM printer is that if the surface has high aspect ratio structures, the printer nozzle might not be able to print evenly without maybe damaging the structures on the Si wafer.

The polymer used with the FDM 3D printer was Acrylonitrile Butadiene Styrene (ABS). Available nozzle opening sizes range between 0.1 mm and 0.4 mm in diameter. The chosen nozzle opening was 0.4 mm in diameter. The smaller the nozzle, the thinner each printed layer would be, which will increase

the printing time. The 3D printer was first calibrated without the Si wafer. Thereafter the Si wafer was placed onto the printer bed, and the software was adjusted to start printing at a height of $500\ \mu\text{m}$ (the height of the Si wafer). The wafer was then sprayed with hair spray that leaves a thin layer of water soluble polymer Polyvinyl alcohol (PVA) on the wafer. The PVA polymer enhances adhesion of the ABS to the wafer and also protects the apertures from ABS, since any ABS residues can be washed away with water. The shadow mask thickness was $100\ \mu\text{m}$ and a total of $60\ \text{mg}$ of ABS was used. The total cost of the ABS plastic and the running time of the 3D printer was less than one euro cent. The printing time was $4\ \text{min}$ and the bed temperature was 70°C .

4. Masking with 3D shadow mask

The Si wafer with the 3D printed shadow mask were rinsed with IPA, followed by a water rinse. The wafer was placed in the FHR MS 150 sputtering tool. A layer of $44\ \text{nm}$ Ti and $200\ \text{nm}$ Au were sputtered on top (Fig. 2a and b). The wafer with the shadow mask was immersed in an acetone bath and agitated for one hour. The ABS shadow mask was then released, Fig. 2c.

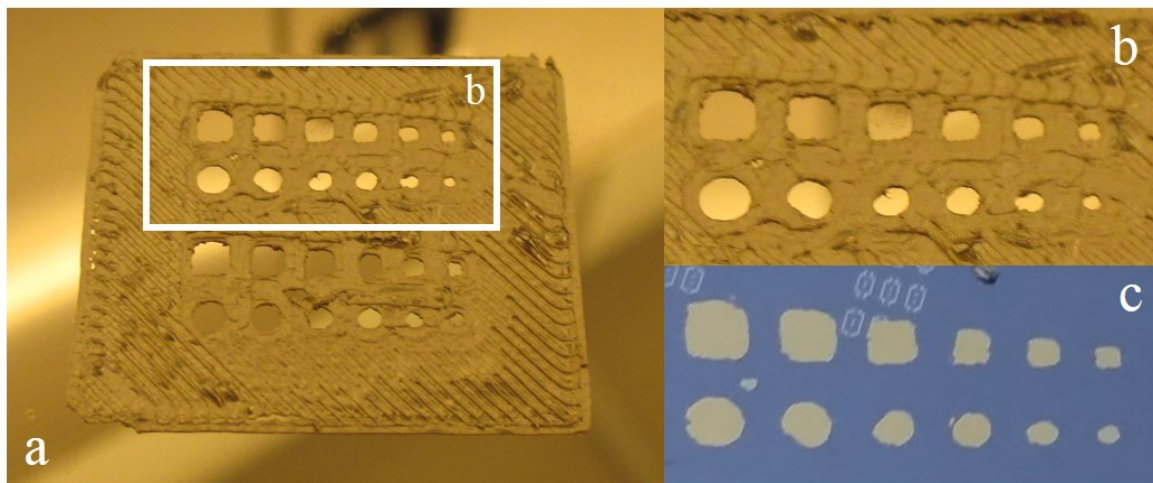


Figure 2: a) The 3D printed shadow mask on the Si wafer after Ti/Au sputtering. b) A close-up of the apertures in a). c) The Ti/Au patterns after the 3D printed shadow mask was released.

5. Evaluation of pattern transfer to the Si substrate

Fig. 3 shows the printed aperture before Ti/Au sputtering, and the Au patch generated from that aperture after lift-off. The widths of the Au patches were measured and compared to the design widths and the printed widths, see Tab. 1. The shadow mask aperture widths are overall smaller than the design, however the Au patches are bigger than the shadow mask aperture widths. The biggest Au patches were between -14% and $+2\%$ of the designed target width, and the smallest Au patches were between -32% and -20% of the target width.

6. Discussion

The printed aperture widths were smaller than the design, probably due to smudging of the ABS during printing. However, the Au patterns transferred to Si wafer were larger than the printed aperture widths thus compensating partly this. The largest Au patch were between -14% and $+2\%$ of the target width. The smallest Au patches were between -32% and -20% of the target width. The 3D printer prints more accurate for the larger structures than the smaller structures. This however can be adjusted by

Table 1: The average widths and standard deviation measured on the printed mask and the patterned Au are compared to the design width.

Design width (mm)	2.0	1.8	1.6	1.4	1.2	1
Printed width (mm)	1.79 ± 0.15	1.61 ± 0.16	1.37 ± 0.17	1.18 ± 0.03	1.01 ± 0.19	0.76 ± 0.17
Au width (mm)	1.87 ± 0.15	1.66 ± 0.14	1.41 ± 0.16	1.24 ± 0.09	1.04 ± 0.12	0.74 ± 0.06

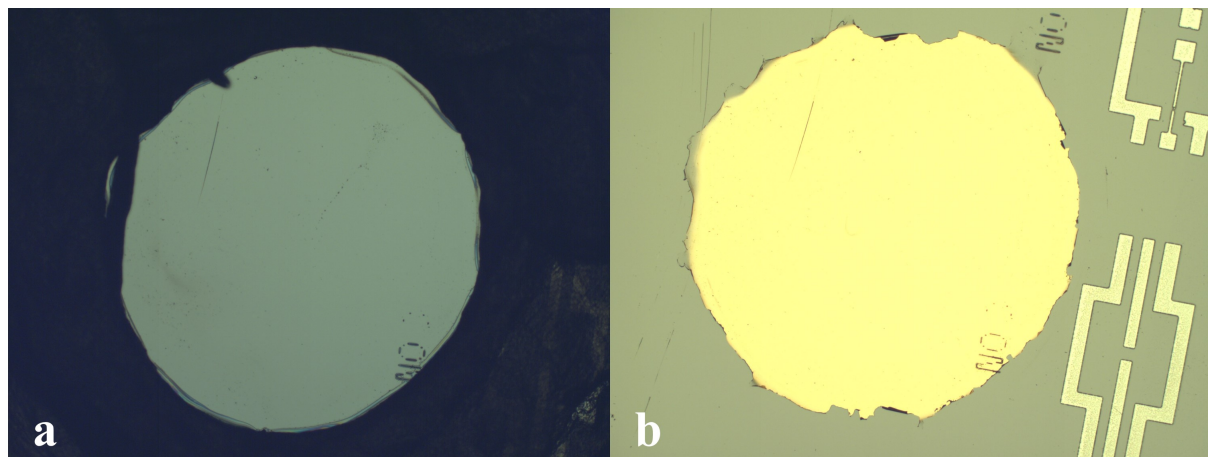


Figure 3: a) Printed aperture. b) Au patch produced from that aperture.

using a one of the smaller nozzle diameter. A smaller nozzle diameter will reduce the flow of ABS, thus resulting in less smudging during printing. A smaller nozzle diameter will also give a better resolution and thinner printing layers, which will also reduce smudging. A 0.25 mm nozzle diameter will print the same structure in about 9 min . The deviation from the target width can also be compensated for in the design.

7. Conclusion

A 3D printed ABS shadow mask prototype was printed directly on the Si wafer. The shadow mask and Si wafer were sputtered with Ti and Au and the shadow mask was released from the Si wafer by immersion into an acetone bath. The Au patches were closer to the target for the wider patches and more off target for the smaller patches. However, this can be adjusted with a smaller nozzle and a compensated design. The process is a low temperature process suitable for electronic structures not needing very high resolutions, the printing time is fast and the cost of the shadow mask is less than one euro cent.

Acknowledgments

The authors would like to acknowledge the Swedish Research Council VR Grant Number C0466101, the Swedish energy council, and the Chalmers production area of advanced science for funding of the reported work.

References

- [1] Dohler G H, Hasnain G and Miller J N 1986 *Applied Physics Letters* **49** 704 ISSN 00036951 URL <http://scitation.aip.org/content/aip/journal/apl/49/12/10.1063/1.97573>
- [2] Brugger J, Andreoli C, Despont M, Drechsler U, Rothuizen H and Vettiger P 1999 *Sensors and Actuators A: Physical* **76** 329–334 ISSN 09244247
- [3] Tixier A, Mita Y, Gouy J P and Fujita H 2000 *Journal of Micromechanics and Microengineering* **10** 157–162 ISSN 0960-1317 URL <http://stacks.iop.org/0960-1317/10/i=2/a=310?key=crossref.a132af2290fa5324ea79da2d297e0ee8>
- [4] Apanius M, Kaul P B and Abramson A R 2007 *Sensors and Actuators, A: Physical* **140** 168–175 ISSN 09244247
- [5] Kolari K 2008 *Sensors and Actuators A: Physical* **141** 677–684 ISSN 09244247
- [6] Keller S S, Bosco F G and Boisen A 2013 *Microelectronic Engineering* **110** 427–431 ISSN 01679317
- [7] Sowmya N S, Oraon N, Sen S and Rao M 2015 *2015 IEEE International Conference on Electronics, Computing and Communication Technologies (CONECCT)* (IEEE) pp 1–5 ISBN 978-1-4799-9985-9 URL <http://ieeexplore.ieee.org/lpdocs/epic03/wrapper.htm?arnumber=7383925>
- [8] Khan S, Dang W, Lorenzelli L and Dahiya R 2015 *2015 XVIII AISEM Annual Conference* (IEEE) pp 1–4 ISBN 978-1-4799-8591-3 URL <http://ieeexplore.ieee.org/lpdocs/epic03/wrapper.htm?arnumber=7066786>